

DETECTION OF BREAKWATER FAILURE MODES FROM PHOTOGRAMMETRIC DERIVED POINT CLOUDS – A CASE STUDY FOR BUNBURY PORT, WESTERN AUSTRALIA

P. Helmholtz¹, L. Boyle², B.E. Tily-Laurie³, D. May⁴, G. Singh⁵, J. Hogben⁶, Y. Ren⁷, Q. Li⁸, D. Belton⁹, S. Khaksar¹⁰ and S.J. Snyman¹¹

^{1,2,3,4,9}*Spatial Sciences, School for Earth and Planetary Sciences, Curtin University, Australia*

^{5,7}*Innovation Central Perth, Curtin University, Australia*

^{6,11}*Southern Ports Authority, Australia*

^{8,10}*Curtin Cisco Centre for Networks, School of Electrical Engineering, Computing, and Mathematical Sciences, Curtin University, Australia*

Abstract

The concept of a digital twin is increasingly applied to a wide range of physical assets as it offers spatial contextualisation, temporal contextualisation, simulation, and optimisation. For the Southern Ports Authority (SPA) of Western Australia one important asset class is breakwater walls. SPA has implemented a spatial contextualisation for their breakwater facilities using a Geographic Information System (GIS) including the breakwater wall condition. This proof-of-concept study aims to validate that timely mapping of breakwater conditions using Unmanned Aerial Vehicles (UAV) and the information derived from the images captured by UAVs is possible. Three failure modes have been investigated using single and multiple epoch data. The failure modes are slope defects, breach or loss of crest elevation and armour movement or loss of armour interlocking. The highest potential for an automatic assessment was concluded for the Breach or loss of crest elevation failure mode. Armour movement or loss is likely to be detected as well, as long as the point spacing of the point clouds in different epochs is comparable. Further investigations are required for the loss of armour interlocking as well as for multi-epoch slope defect assessment. Hence, while it is a proof-of-concept study only, it is the first step to develop a more automated assessment of breakwater walls. Consequently, this data can then be used for simulation and optimisation and the integration of the data in business processes, i.e., the maintenance cycle for the breakwater walls.

Keywords:

Breakwater, Failure Modes, UAV, Point Cloud, Point-To-Point Comparison, Point-To-Model Comparison

1. INTRODUCTION

The concept of a digital twin is increasingly applied to a wide range of physical assets. It integrates facility information into a structured information model, providing an interface for users to access, navigate and engage with asset information via an immersive digital experience. The Southern Ports Authority (SPA) of Western Australia aims to implement a digital twin for their major assets, namely the Ports of Bunbury, Albany, and Esperance [12].

A digital twin offers spatial and temporal contextualisation, simulation and optimisation as well as progress integration. It should be presented in a visualisation layer that delivers the immersive environment for end users to interact with information linked to the digital asset. The digital twin can also be used to display and assess the condition of the breakwater walls and their failure mode ranks [2] [4].

Spatial contextualisation focuses on the information connected to the physical asset enabling users to navigate through the asset information. An implementation can be done using Geographic Information Systems (GIS) or Building Information Models (BIM) [5]. SPA has implemented a spatial contextualisation of the Port of Bunbury using GIS for their breakwater facilities. More specifically, breakwater (or seawall) condition is mapped including information such as the seawall type, chainage points and severity of the failure modes [6].

This project aims to validate that timely mapping of breakwater conditions is possible using Unmanned Aerial Vehicles (UAV) and the information derived from the images captured by UAVs [15]. The project is a proof-of-concept study and the first step to hopefully allowing an automated assessment of breakwater walls after major weather events, such as storms, in the future. Consequently, this data can then be used for simulation and optimisation (e.g., predictive models for future weather events) and the integration of the data in business processes (e.g. logistic movements and space constraints) [19].

After reviewing existing literature about the assessment of breakwater walls using UAV and terrestrial laser scan data, the different failure modes for breakwaters are presented next. Then, the study area and the data are introduced. The different methods for the processing of the data to investigate the failure modes are discussed and it is concluded which method is useable for the assessment of different failure modes [22] [26]. Finally, the results of a proof-of-concept analysis for three different failure modes are presented and discussed. The paper will close with a conclusion.

2. AIMS AND OBJECTIVES

The aim of this project is to review breakwater failure modes and the possibility to establish an automated assessment workflow. Methods will be established and evaluated for some of the failure modes which were identified to offer the opportunity for automated assessment. For the automated assessment of the failure mode photogrammetry-derived point clouds are used. The proof-of concept investigation and its output are assessed using both numerical and visual methods. The implementation involves the segmentation, registration and comparison of point clouds created from UAV data and spatial models of the breakwater crest and armour as well as the use of profiles derived from the UAV data. The automated comparison of the static model and various epochs of point clouds will allow the determination of breakwater

degradation over time, and especially after severe weather events. This will greatly simplify the workflow for ports authorities to determine breakwater failure and decrease response time regarding breakwater damage.

3. RELATED WORK

Most of the recent papers use photogrammetric point clouds derived from images taken from an UAV or LiDAR. Image derived point clouds were used in Lemos et al. [11] more specific a DJI Inspire V1 Pro, Sousa et al. [20] used a PhaseOne camera iXM-50 mounted on a DJI Martice 600, González-Jorge et al. [8] used a Mikrokopter Okto XL equipped with a Sony Nex7 camera. LiDAR systems were used by Ueno et al. [23] more specific a DJI Martice 600 Pro and Hokuyo UTM30LX airborne laser scanning system and Gonçalves et al. [7] used a terrestrial laser scanner in combination with a DJI Phantom 4 RTK (P4RTK).

Most of the Australian breakwaters are rubble mound structures. The armour rock forming the breakwater are irregular and usually not larger than 1.5m in diameter. In contrast, existing literature dealing with the automated assessment of breakwater walls are often located in Portugal [7] [11] [20] and Spain [8] focusing on large (2m or larger) square concrete blocks. These blocks have very regular shapes which makes it easy to fit planes and to determine, e.g., the direction of the block. In contrast, the rubble mound structures have very different geometric characteristics and due to their irregular shape, it is nearly impossible to model them in the same way as the regular shaped concrete blocks.

While some studies are not using the point cloud itself for the assessment but derived data such as profiles [7], most of the publications use the point cloud itself. For the data processing a traditional workflow is usually followed. Ueno et al. [23], Sousa et al. [20] and Gonçalves et al. [8] broke the steps down in outlier removal, initial alignment, fine alignment and finally change detection. While off-the-shelf products can be used such as CloudCompare, a more customised process can be achieved using the Point Cloud Library (PCL) and open3d library.

Rusu [18] states that the comparison of points within a cloud must depend on geometric metrics and characteristics that extend beyond merely coordinates. Such characteristics are measured from a region of points rather than a singular point. Therefore, the concept of a 3D point with singular coordinates is replaced by the concept of a local descriptor. By including surrounding neighbours of a point, surface geometries can be computed, and patterns can be more easily predicted. This indicates that the geometric characteristics of the breakwater crest should be taken advantage of.

If different parts of breakwaters are to be assessed, segmentation as an additional pre-processing step must be applied. For instance, the crest region is unique compared to the armour point cloud in that it resembles a horizontal plane and has a relatively high level of smoothness. Alternatively, the region has a distinct lighter colour than other regions on the wall and consequently, segmentation based on colour and/or texture could be optimal.

Grilli et al. [9] lists various point cloud segmentation methods including edge-based, region growing, model fitting, hybrid, and machine learning techniques. Rabbani et al. [16] lists edge-based,

surface-based, and scanline-based segmentation methods and utilised normal estimation and region growing to segment sets of point clouds within industrial sites. It was concluded that smooth areas had been successfully achieved and over-segmentation had been avoided.

Edge-based methods, although allowing rapid segmentation, tends to sacrifice accuracy in noisy cases and cases with uneven density, which is true of the acquired breakwater point clouds. Moreover, edge-based segmentation often results in disconnected edges which require a difficult additional step of edge connectivity.

Region growing algorithms utilise selected seed points and grow regions based on selected characteristics, often based on neighbouring points. However, it does tend to suffer from a lack of robustness and large computation times [24]. In the case of breakwater crests, the robustness is not such a large issue as most crests have a similar plane-like shape. Region growing processes are superior compared to clustering or thresholding approaches for colour-based segmentation as they account for both colour similarity and spatial proximity of clusters [21].

For crest depression assessment, the segmented crest is compared with a 3D model of the crest and armour supplied by SPA. The first obstacle in achieving this is cloud registration. A simple vector transformation followed by the Iterative Closest Point registration algorithm (ICP) is utilised to align the cloud and model. The ICP algorithm is a common geometric alignment technique which repeatedly compares corresponding points between two meshes and minimizes its error [17].

The distances between the crest points of the cloud and the supplied model are calculated with a cloud-to-mesh distance method between the segmented cloud and the 3D model where the closest distance between each point to the mesh surface is computed and plotted [13]. In this paper, we will follow the usual used processing pipeline, i.e., segmentation, initial alignment, fine alignment, point cloud comparison or to derive profiles for further assessment.

4. BACKGROUND

4.1 BREAKWATER FAILURE MODES

An overview of all breaches is provided in [22]. Reports usually refer to this source. This definition below as well as the figures were also taken from this reference [22].

Breach or loss of crest elevation (Fig.1) refers to a reduced height across a section or sections of a breakwater structure. More specifically, a breach is a depression or gap in the crest. A loss of crest elevation can occur because of a settlement of the structure or its foundation.

When the underlayer or core stones of a breakwater wall can be readily seen through gaps between the primary armour rocks then core exposure is present (Fig.2). Not secured, the core exposure will lead to core loss.

Armour movement or loss is the cases when an armour is lost or moved from a rubble mound structure and consequently will lead to loss of armour interlocking and slope defects (Fig.3).

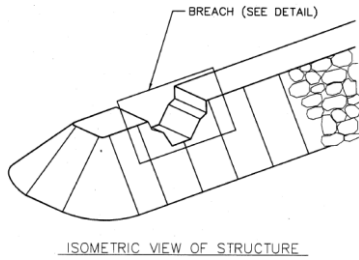


Fig.1. Breach of breakwater structure [22]

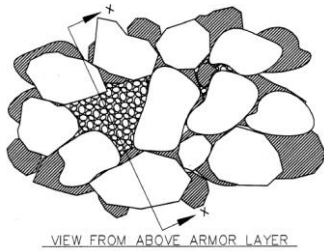


Fig.2. Core Exposure [22]

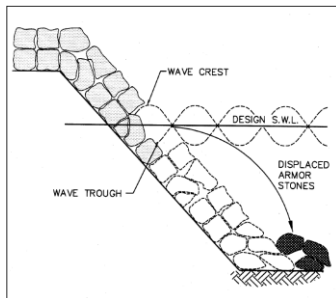


Fig.3. Armour loss [22]

Armor interlock refers to the physical containment by adjacent armors. The individual armor rocks tend to be held together and therefore act as a larger interconnected mass. Interlocking armor rocks lead to increasing the robustness of the structure. Without interlocking armor rocks the integrity of the breakwater structure is compromised (Fig.4).

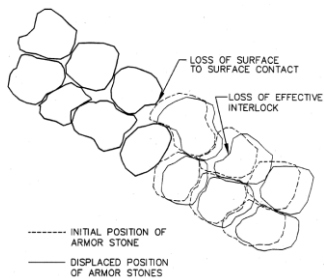


Fig.4. Loss of Armour Interlocking [22]

Armor quality defects refers to the damage and/or deterioration of individual armor rocks. There are several categories of armor rock defects including, rounding, cracking, and fracturing etc. [22].

Slope defect means that the shape or angle of the side slope is effectively changed. Reasons can be armor loss or settlement over a large enough area of the structure. Slope defects generally

occur in the form of either slope steepening (Fig.5, left) or sliding steepening (Fig.5, right).

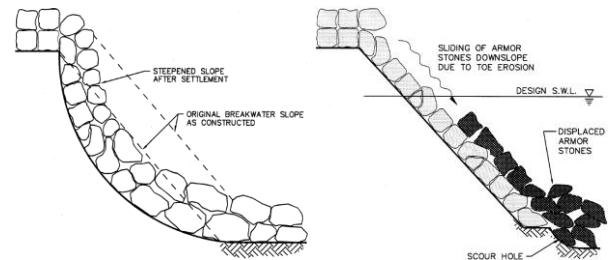


Fig.5. Slope Defects [22]

4.2 ASSESSMENT OF BREAKWATER FAILURE MODES

A rating system is used to assess the structures' conditions. Based on [22], there are overall 7 condition ratings. The condition ratings with their index values are: New (90 – 100), Excellent (80 – 89), Good (65 – 79), Fair (50 – 64), Marginal (35 – 49), Poor (21 – 34) and Failed (0-20).

Assessment is usually performed along chainage points. The distance between chainage points for the Port of Bunbury is 10m. The assessment is usually performed by visual walkover inspections of the above water portions. If required, land, hydrographic and aerial surveys are used to inspect the underwater section of breakwater structures. Aerial surveys can be impacted by white water washes and waves; hydrographic surveys can be impacted by very shallow water depths.

The condition assessment is then used for the identification of key risk failure areas which are used to prioritise the schedule for maintenance works.

4.2.1 Study Area:

The study area is the Port of Bunbury located south of Perth in Western Australia. The dominant breakwater structure is rubble mound structures which have been constructed between 1934 (Inner Harbour Groyne) and 2015 (Koombana Beach Revetment). All structures are listed in Table.1; their location is shown in Fig.6.

Table.1. Breakwater structures at the Port of Bunbury from (m p rogers and associates pl, 2020).

Structure location	Location	Wall #	Year of Construction
Inner Harbour	Inner Harbour Groyne	1	1934 - 1936
	Inner Harbour East Training Wall	6	App 1976
	Berth 4 Revetment	-	App 1976
	Inner Harbour East Revetment	3	1996
	Inner Harbour West Revetment	4	1996
	Inner Harbour Berth 3	-	App 1976
	Inner Harbour West Training Wall	5	App 1976
	Koombana Beach	-	2015

	Revetment		
Outer Harbour	Casuarina Harbour Inner Revetment	-	App. 1996
	Outer Harbour Sand Trap Grove	8	1949 - 1952
	Outer Harbour Main Breakwater North	7b	Various sections 1896 - 1952
	Outer Seaside Main Breakwater	7c	App 1970
	Outer Harbour Groyne	7a	1948 - 1951

The data used are photogrammetric derived point clouds. The images were captured at two different time points nearly one year apart. It must be highlighted that the first epoch data capture was performed using a strong geometry, i.e., using multiple angle views along the breakwaters. In contrast, the second capture was a non-specific mapping double grid flight pattern using a single flight height and a nadir view camera and no ground control. An overview of the point cloud data is provided in Table.2.



Fig.6. Breakwater structures' locations within the Port of Bunbury. Image source (m p rogers and associates pl, 2020).

Table.2. UAV point cloud data - overview

	Epoch 1	Epoch 2
Date	May 2021	March 2022
UAV	DJI Phantom IV	DJI M300
Flight pattern	A combination of orbit and grid flights	Double grid, single flight height
Control	Control points established using RTK	Drone RTK using a base station
Processing software	Metashape	SiteScan
Camera calibration	f, xp, yp, k1-k3 (radial lens distortion), p1, p2 (decentering distortion)	

It must be noted that the point spacing in point cloud 2 for some of the walls was much larger than in point cloud 1 (see Fig.7). If this is the case for any of the comparisons in this paper, it will be explicitly mentioned.

Furthermore, the 2021 Rubble Mound Structures Condition Inspection and Asset Management Plan was provided. The Asset Management Plan contains general information about the structures such as shown in Table.1 but also the scores of all breakwater failure modes. Scoring was provided for chainage points in an interval of 10m.

No drawings or as built information of the breakwater structures are available. Hence, for the failure mode assessment, only general guidelines related to the required slope could be used.

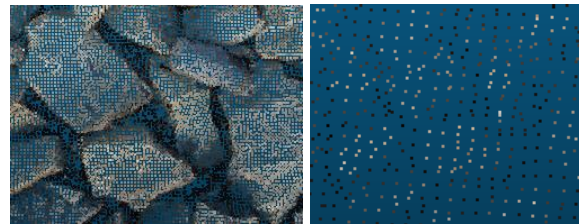


Fig.7. Comparison of point spacing in epoch 1 (left) and epoch 2 (right) for wall 5. Both images show the same and equal sized area

5. METHOD

The only input data for the inspection are the point cloud data as presented in Table.2. As point cloud data from two epochs were available, there are two options for the assessment of failure modes:

- Single epoch analysis
- Epoch-to-epoch comparison

For the single epoch analysis, a single point cloud can be used to extract geometric features such as planes and contours fitted to the point clouds. Then extracted contours could be used to assess slope and consequently slope defects as well as core exposure. On the other hand, a fitted plane could be used to compare the distance of the points in a point cloud to the extract plane and consequently it will be possible to detect depressions or gaps of the crest of a breakwater structure.

In contrast, epoch-to-epoch comparisons allow the comparison of point clouds from different epochs. Using this method, armour loss or displacement as well as slope defects should be able to be detectable.

The Table.3 shows a summary of the different failure modes and the prediction if it is possible to assess them based on a single epoch or epoch-to-epoch assessment. The only failure mode which is believed to be not able to be detected using point cloud data is the armour quality defect. Image data is likely to be utilised to assess this defect.

Table.3. Failure mode assessment likelihood using a single epoch or epoch-to-epoch analysis

Failure mode	Single Epoch Analysis	Epoch-to-Epoch comparison
Breach or loss of crest elevation	Possible	Possible
Core exposure or loss	NA	Possible
Armour movement or loss	Possible	Possible
Loss of armour interlocking	NA	Possible
Armour quality defects	NA	NA
Slope defects	Possible	Possible

For this proof-of-concept study, the point cloud processing methods as implemented in CloudCompare has been utilised [3] as one method. In addition, an implementation using Point Cloud Library (PCL) and open3d library was implemented for the assessment of crest elevation to achieve a higher degree of automation.

5.1 FAILURE MODE DETECTION WITH A SINGLE EPOCH - STRING LINE EXTRACTION FOR SLOPE DEFECT ASSESSMENT

Along the chainage points, narrow point cloud sections are extracted. Those are also referred to be cloud slices. From each slice a 2D contour along the section is extracted. There are several methods available to fit the contour, e.g. to align with the lower or the upper part of the slice. For this research the contours are fit to lower part aiming to extract the breakwater walls and “removing” any vegetation on the breakwater walls. More details about the contour extraction are available on pp 122 [3].

For each extracted contour, it is then possible to derive the slope of it. Consequently, the slopes belonging to the same breakwater wall can be used to calculate a mean slope for the wall, their standard deviation, maximum and minimum slope values as well as the median slope.

5.2 FAILURE MODE DETECTION USING EPOCH TO EPOCH COMPARISON (METHOD 1)

For the epoch-to-epoch comparison, it would be possible to compare the point clouds covering the whole Port of Bunbury. However, as assessment is performed along chainage points, the point clouds were segmented in sections. The section boundaries are aligned with chainage points.

Generally, the epoch-to-epoch analysis is broken down into two steps: the rough alignment of the clouds followed by a fine alignment. A rough alignment is not required in our case as the UAV derived point clouds are georeferenced. Consequently, only a fine alignment was performed. This processed is also referred to be a Cloud Registration.

A Cloud Registration tries to minimise the distance between two different point clouds, the underlying algorithm is the Iterative Closest Point (ICP) algorithm. The ICP allows to adjust for scale. This option was not applied to the datasets as both point clouds are metric point clouds. More details are available in [3].

Then, the distance between the two registered point clouds can be calculated in several ways – usually using either the cloud-to-cloud distance or the cloud-to-model distance. For both distance measures, a reference point cloud must be nominated.

The cloud-to-cloud method will compute the distances of each of its points relatively to the reference cloud simply using the nearest neighbour distance (using a kind of Hausdorff distance algorithm, [3]). The issue is that the nearest neighbour is rarely the actual nearest point on the surface represented by the cloud.

This issue is overcome when using, the cloud-to-model distance. In this case a local model is fitted through the reference point cloud. While there are several methods for the local modelling available, the Least Squares Plane fitting method has been applied for this research. Different numbers of points to fit

the plane are tested for this research. For more details, check pp. 106 [3].

Again, a heat map is created based on the calculated distances and is used to present the results. The scalar field which is shown in the heat map has a lower and upper saturation point. Standard saturation points are at the minimum and maximum distance values which gives a visually even colour scale distribution (see Fig.8 top). However, as we are especially interested in highlighting small changes, the upper saturation point is set to 10 cm (0.1m) (see Fig.8 bottom) allowing much better differentiation of small changes.

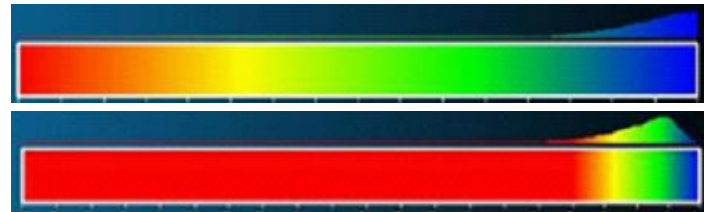


Fig.8. Impact of changing the scalar field saturation point to 0.1m (bottom) compared to saturation points set to maximum (top)

5.3 FAILURE MODE DETECTION USING EPOCH TO EPOCH COMPARISON (METHOD 2)

An alternative method for the assessment of epoch-to-epoch comparison was implemented using the Point Cloud Library (PCL) and open3d library. The main focus is on the crest assessment. The general workflow is shown in Fig.9. After outliers have been removed, the crest points are segmented using a combination of region growing and the merging of resulting regions. After the crest cluster is extracted, the crests of a point cloud and a model derived from a second point cloud is aligned. Finally, the point cloud distances are calculated.

As each point cloud contains multiple millions of points, pre-processing is first performed. Outliers can distort the computation of local point features such as normal and curvatures, which may in turn distort the registration between the point cloud and the 3D model [18]. Statistical outlier removal is implemented over two iterations, the first of which calculates the mean and standard deviation of the distance of each point with its nearest 100 neighbours. The second iteration classifies points as inlier or outlier depending on a distance threshold equal to $\mu \pm \alpha \cdot \sigma$, where α is set to 1. Any point which falls outside this threshold is removed [14].

Then, the number of points is decreased via voxel grid downsampling to decrease processing times of segmentation and cloud registration. Downsampling preserves the spatial distribution of the point cloud whilst decreasing its spatial density [1]. All points within each voxel are approximated to its centroid. In this case the voxel size is set to 50cm, which is enough to preserve the shape of the breakwaters.

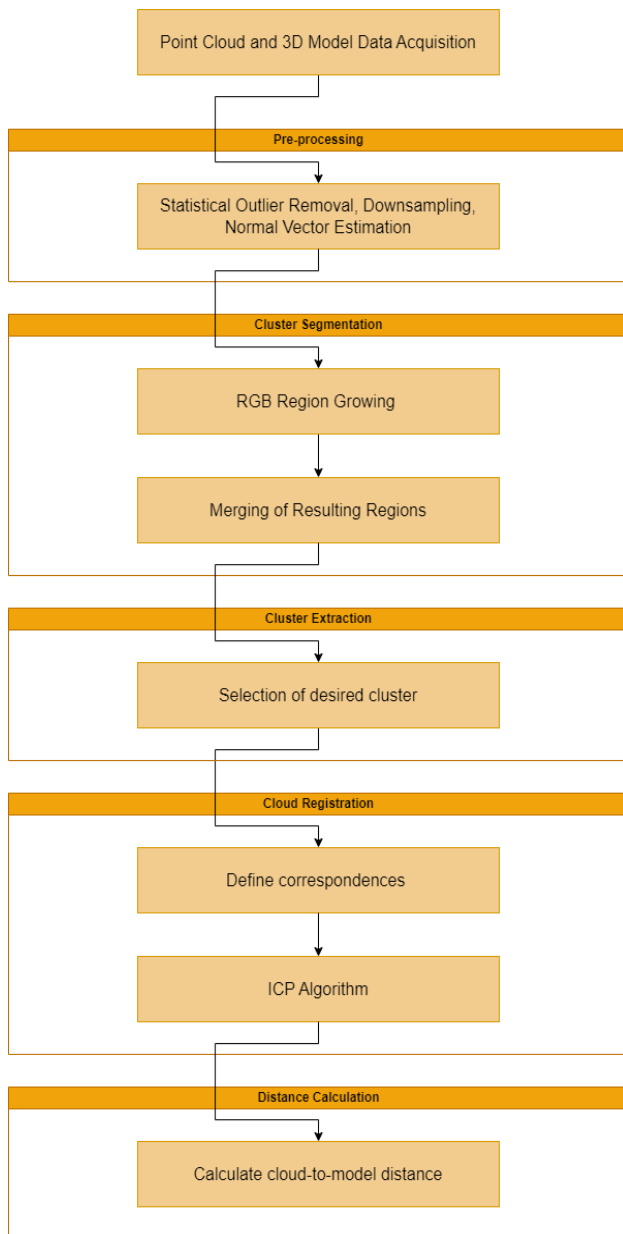


Fig.9. System architecture for automated crest depression assessment

Colour-based region-growing segmentation is performed for the segmentation of breakwater crests. The algorithm is similar to the traditional region-growing segmentation algorithm except that region growth is conditional upon changes in colour rather than changes in normal vectors between nearest neighbour points [18]. Changes in colour, referred to as colorimetric difference, is measured by the spatial distribution of colours, which can be thought of as the Euclidean distance between RGB colours [21] [25].

The utilised algorithm consists of two major stages [14]:

- 1) Region growing based on criteria that consider colour similarity and spatial proximity; and
- 2) Merging of the resulting regions based on colorimetric similarity and number of points in a cluster.



Fig.10. Wall 1 outliers with $\alpha = 1$ and nearest neighbours set to 100

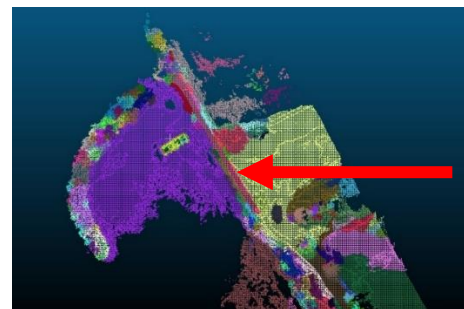


Fig.11. Pink strip down middle of breakwater defines crest as shown by red arrow. Segmentation done with distance threshold parameter set to 5, colorimetric difference between points set to 8, region merging threshold set to 5. Higher values for these parameters equate to a higher allowable colorimetric distance for both points and regions, and therefore a lower level of segmentation and vice versa.

The first stage of the algorithm initiates a new region from a single labelled point. When encountering an unlabelled point, a new region is created and pushed to a stack. When a point is popped from the stack, region growth occurs by finding its k-nearest neighbours within a certain distance threshold via a kd-tree search algorithm and determining the colorimetric similarity of the neighbouring points. The process continues until the stack is empty and rough regions are assigned.

The second stage is helpful for preventing over or under-segmentation and refining the segmented regions. Neighbouring clusters with a small colorimetric difference are merged based on a mutable parameter, followed by a cluster size filter. In this case, the allowable cluster size is set to be between 100 and 100000 points [25].

The segmented crest must be extracted to make a cropped cloud and registered with the supplied 3D models for the final crest depression computation. First, the model is converted to a point cloud by making each of its vertices a point. A point-to-point algorithm is then implemented which iterates over two stages [13]:

- 1) Define set of points as correspondences on the meshes transformed by a calculated transformation matrix; and
- 2) Update this transformation matrix by minimizing an objective function calculated from the set of corresponding points.

The objective function used in this study is defined by Besl and McKay (1992):

$$E(t) = \sum_{(p,q) \in K} \|p - Tq\|^2 \quad (1)$$

where $E(T)$ is the objective function, (p,q) is a correspondence point, and T is the transformation matrix to be optimized as the objective function is minimized. Three corresponding points on both the point cloud and the model cloud are manually selected by the user and utilised for cloud registration.

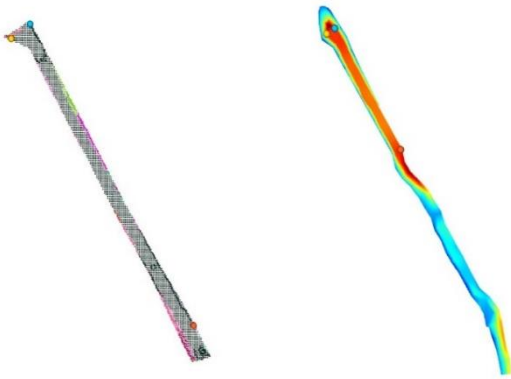


Fig.12. Three correspondences chosen on cropped cloud (left) and model cloud (right)

A threshold parameter representing the maximum allowable distances between the corresponding points on both meshes is also set. The lower this parameter, the closer the meshes must be for a good fitness result. As the model and clouds for this study are relatively simple, only consisting of the breakwater crest and armour, this parameter is not extremely significant and is set to 3 cm. Over each iteration of the algorithm the root-mean-square error (RMSE) between the two meshes is calculated [13].

After cloud registration, the distances between the crests on the cropped cloud and the model cloud are calculated. However, signed distances are required to determine whether crest depression has occurred. To achieve this, a method is introduced in which the original mesh is utilised; if a point on the cropped cloud is within the mesh, an occupancy variable is set to 1 and the distance is set to a negative value. Similarly, for points outside the mesh, the occupancy variable is set to 0 and the distance is positive. Therefore, a cloud-to-mesh distance is utilised in which the closest distance from each point in the cropped cloud to the mesh surface is calculated [13]. Although the model cloud consists of crest and armour, as the cropped cloud only contains the segmented crest, only the crest points will be considered in this distance calculation.

6. PROOF OF CONCEPT ANALYSIS

While armour movement or loss should be able to be detected using a single epoch as well as an epoch-to-epoch assessment (see Table.3), it was decided that only the epoch-to-epoch approach is used for this failure mode due to the condition of the breakwater walls in the Port of Bunbury.

For this study, this leads to the following breakwater failure modes to be assessed using a single epoch only:

- Slope defects

- Breach or loss of crest elevation

And for the epoch-to-epoch assessment the aim is to assess the following breakwater modes:

- Armour movement or loss
- Loss of armour interlocking

6.1 SINGLE EPOCH ASSESSMENTS - SLOPE DEFECTS

The failure mode was tested using the following breakwater walls:

- Inner Harbour Groyne (wall 1)
- Inner Harbour East Revetment (wall 3)
- Inner Harbour East Training Wall (wall 6)
- Outer Harbour Groyne (wall 7a)
- Outer Harbour Main Breakwater North (wall 7b)
- Outer Seaside Main Breakwater (wall 7c)
- Outer Harbour Sand Trap Grove (wall 8)

Examples for the derived contours are provided in **Error! Reference source not found.** Each of the derived contours align with chainage points. It is clearly visible that the main challenge is that the contours are not smooth and are heavily impacted by the placement of armour rocks. Hence, it is not possible to simply extract the slope of those contours.

Instead, points which are likely to present the breakwater slope are manually selected. The selection is impacted by the point cloud detailing and the lack of clarity in areas of loose rock such as the beaches. Nevertheless, due to the human interaction it is possible to derive the slope and consequently analyse them along the different chainage points of walls. These results are summarised in Table.4. The slope measures are presented in Grade/Slope (1m hz).

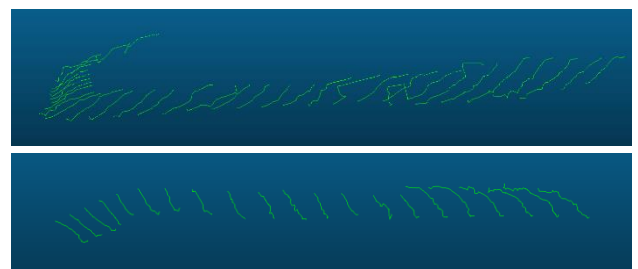


Fig.13. Contour derived of Wall 6 (top) and Wall 8 (bottom)

The Table.4 shows that Wall 1 has the largest Standard Deviation (Std) in the slopes. Contributing to the large Std of Wall 1 is also that this is the wall with the smallest minimum slope (min) with a value of 0.001. In contrast Wall 4 has the maximum slope (max) with a value of 0.958. The median slope values show that Wall 5A and Wall 7 are very similar (0.550 and 0.529). Wall 4 is the steepest wall (0.753) and Wall 1 the least steep (0.214).

Table.4. Slope (Grade/Slope (1m hz)) statistics of five different walls

	Wall 1	Wall 2	Wall 4	Wall 5A	Wall 7
# chainages	31	32	7	16	21

Mean	0.349	0.347	0.721	0.545	0.510
Std	0.340	0.148	0.199	0.128	0.129
Max	0.935	0.656	0.958	0.813	0.732
Min	0.001	0.034	0.596	0.268	0.247
Median	0.214	0.351	0.753	0.550	0.529

The results in Table.4 have been confirmed by engineer observation. To conclude, while slope measures can be derived, the main challenge is the manual selection of the points along the contours to extract the slope which is unlikely to be a trivial exercise to be automated.

6.2 BREACH OR LOSS OF CREST ELEVATION

The failure mode was tested using the following breakwater walls:

- Inner Harbour Groyne (wall 1)
- Outer Harbour Groyne (wall 7a)
- Outer Harbour Main Breakwater North (wall 7b)

6.2.1 Method 1 – Using the CloudCompare Implementation:

The results are shown as a 95% measurement range in Table.5 and in form of heat maps and histograms in Table.7. Table.5 shows deformations in the sub-meter to meter range. The threshold for Wall 1 and Wall 7a is approximately the same with around 65cm. Wall 7b, a much older breakwater wall, shows a value nearly double of the other walls with 1.285m.

A trend of lower breakwater walls at the end of the crests is visible for all three breakwater walls. The centre section of the crest is always higher than the ends. The strongest lowering is visible in Wall 7b which correlates with the results presented in Table.5.

The Inner Harbour Groyne (wall 1) Fig.in Table.7 shows the impact of not being able to separate between crest and non-crest points successfully. At the southern edge, an elongated area of points with a much lower values compared to other crest points is visible.

Table.5. Assessment of Breach or loss of crest elevation using a single epoch – 95% of the measurements range.

	95% measurement range
Inner Harbour Groyne (wall 1)	0.653m
Outer Harbour Groyne (wall 7a)	0.673m
Outer Harbour Main Breakwater North (wall 7b)	1.285m

This underlines the main challenges faced when modelling the crests by selecting point around the crest edge manually. For future project a baseline 3D vector model of breakwater components will be provided by SPA which can be used for the future point cloud comparison. It is important to use expert knowledge and not just applying automatic segmentation methods as the results will impact the maintenances schedule of breakwater walls and therefore significant cash contributions. Overall, it can be summarised that UAV derived data is very likely to help to automate detection of the failure mode breach or loss of crest elevation.

6.2.2 Method 2 – Using the Point Cloud Library (PCL) and open3d Library Implementation:

For Wall 1, cloud registration between the cropped and model cloud yields the result as shown in Fig.14. The left image of Fig.14 shows that the cropped cloud and model cloud are not initially aligned which explains the need for the basic vector transformation governed by user-selected correspondences. The need for this step in the workflow inevitably introduces an element of random human error, and thereby reduces the reliability of registration. Therefore, it is of the utmost importance that correct and accurate correspondences are selected on both clouds to prevent unwanted variance in results. In future the point clouds and models should be georeferenced, and alignment ensured for greater accuracy in cloud registration. The right subfigure shows the top view of cloud registration, whilst Fig.15 depicts a more revealing side view of the ICP result.

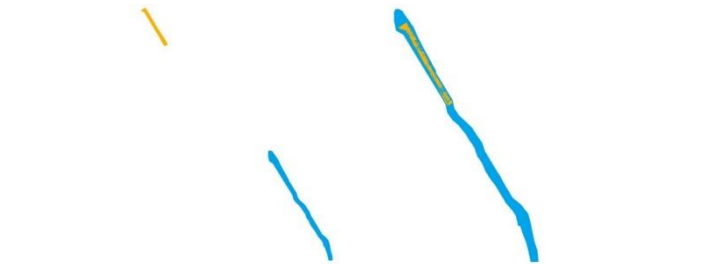


Fig.14. Left – Cropped cloud (yellow) and model cloud (blue) before ICP registration. Right – After registration

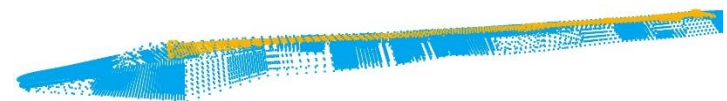


Fig.15. Side view of ICP registration

The cropped cloud (Fig.15) fits neatly on the surface of the model cloud to a large extent. Sections of this cloud can be categorised into either occupant or non-occupant points, indicating the position of the points either within the model cloud or outside it respectively. The head of the cropped cloud consists of non-occupant points as the points are above the model surface. As the head ends, there is a large section of the cropped cloud that is slightly below the model surface and therefore consists of occupant points. Finally, towards the end of the cropped cloud the points are again non-occupants and rise above the surface. The alignment can thus be separated into three sections, indicating that there should be three peaks in the cloud-to-mesh distribution.

Fig.16 illustrates a trimodal distribution of distances between the cropped cloud and model, similar in shape to a normal distribution centred at approximately +0.06m. The three peaks occur at distances of -0.115m, +0.06m and +0.2m. As expected, there are two peaks of non-occupant points, presumably representing the head and tail of the cropped cloud, whilst the single peak of occupant points represents the middle section of the cloud which was within the model surface. Since the cropped cloud has been derived from the downsampled and segmented original cloud of the breakwater wall, there are only 2046 points and thus the same number of computed distances. Fitness between the cropped cloud and model cloud is calculated by the number of inlier correspondences on the cropped cloud divided by the

number of points in the model cloud [13]. As the model cloud contains the crest and armour whilst the cropped cloud contains only the crest, the fitness value is already skewed lower and so the RMSE is the more relevant result.

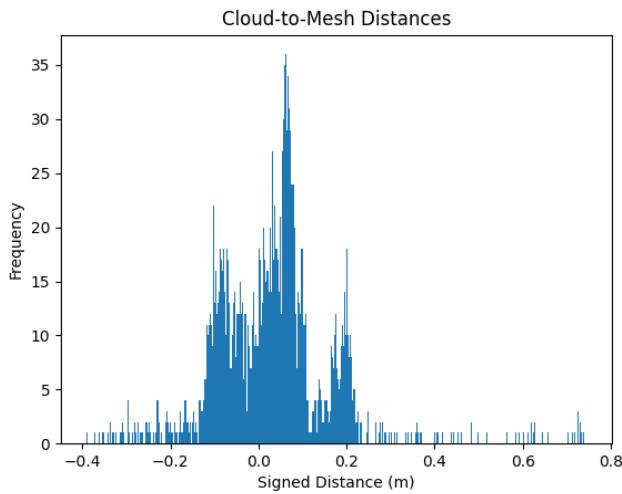


Fig.16. Cloud-to-mesh distance distribution between cropped cloud and model

With careful selection of correspondences, the number of ICP iterations was limited to either 1 or 2, with an average RMSE varying decreasing from 0.07 to a negligible value. However, without such careful selection the number of iterations reached above 20. RMSE was calculated with the maximum allowable distance threshold between the two clouds set to 3 cm. The higher the threshold was set, the greater the number of iterations of the ICP algorithm performed and the higher the obtained error. Essentially, the selection of correspondences and distance threshold were major factors in the ICP result and final RMSE value.

6.2.3 Comparison Method 1 (CloudCompare Implementation) and Method 2 (Point Cloud Library (PCL) and open3d library Implementation):

The cloud-to-model distance result for method 2 as shown in Fig.16 resembles the results from method 1. As displayed in Table.7, the method 1 result also illustrates a largely centred distribution with major peaks at approximately -0.10m and 0.05m. In both methods the distance distribution is centred near zero although in method 1 there is still a significant number of points with distances up to 0.5m. This may be due to the number of points for which the cloud-to-model distance is calculated. As the cropped cloud in method 2 is downsampled, there are a dramatically lower number of points to measure distance from. Therefore, the higher distances outputted by method 1 may be a result of outliers or a lack of pre-processing. The similarity between the two results also indicates that the downsampling step done in method 1 did in fact preserve the shape and distribution of points in the cloud to a large extent.

6.3 EPOCH-TO-EPOCH ASSESSMENTS: ARMOUR MOVEMENT OR LOSS AND LOSS OF ARMOUR INTERLOCKING

The failure mode is tested using the following breakwater walls:

- Inner Harbour West Training Wall (Wall 5)
- Outer Seaside Main Breakwater (Wall 7c)

Two tests have been performed. The first test concentrates on the impact of different distance measures on the calculate cloud differences. The second test investigates the impact of the different point spacing of clouds from different epochs on the nomination of the reference point cloud.

All figures presented in this section show the point cloud comparison results by applying the same colour scale ramp (Fig.17). As mentioned beforehand, the upper saturation point is set to 10 cm (0.1m) which means that all difference values with a value larger than 10cm will be shown in a red colour.

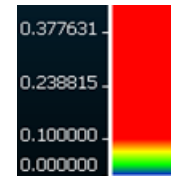


Fig.17. Used colour scale ramp. Units in [m]

6.3.1 Impact of the Comparison Method: Cloud-to-Cloud VS Cloud-to-Model:

The results when applying different cloud comparison methods to Wall 5 is presented in Fig.18. For all results presented in Fig.18, epoch 1 was chosen to be the reference point cloud.

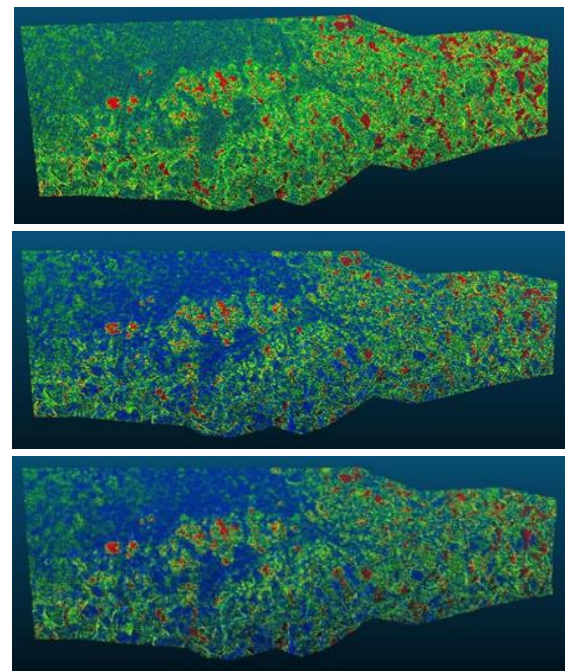


Fig.18. Applying different cloud comparison methods. Cloud-to-Cloud (top), Cloud-to-Model using 6 points for the local modelling (centre), Cloud-to-Model using 18 points for the local modelling (centre)

It is clearly visible in Fig.18 that the cloud-to-cloud method (top) produces the largest differences. The differences are reduced when applying a local modelling method with only minimal differences when applying modelling using 6 and 18 points.

This result is also confirmed when analysing the values of the 95% of all measurements comparison (Table.6). The cloud-to-cloud method has a value of 0.111m in contrast to the cloud-to-model methods with 0.090m when using 6 points and 0.097m when using 18 points for the local modelling. One of the contributing factors is that noise present in a point cloud will impact the results of the cloud-to-cloud methods. The detection of noise and its removal can be a challenging task due to the nature of the objects (armour rocks). Statistical approach may remove noise but also points related to deformation. The cloud-to-model method partially overcome the issue by introducing smoothing. Overall, it can be concluded that the cloud-to-model method will present a more precise reflection of the true difference which has been confirmed by many publications [10].

6.3.2 Impact of the Different Point Spacing on the Nomination of the Reference Point Cloud:

When using the same wall as in previous test but using point cloud 2 as reference point cloud then the results are slightly worse. The value for the cloud-to-cloud method is 0.297m (compared to 0.111m), for the cloud-to-model method using 6 points is 0.103m (compared to 0.090) and using 18 points is 0.109m (compared to 0.097m). The reason being that the point spacing of epoch 2 is slightly less dense than of epoch 1.

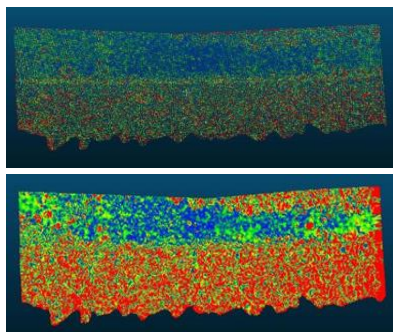


Fig.19. Local Modelling using 6 points. Use of epoch 1 as reference point cloud (top) and use of epoch 2 as reference point cloud (bottom)

This result is confirmed when analysing the point clouds of Wall 7c. The spacing of the epoch 2-point cloud is so low (Fig.7) that a cloud-to-cloud comparison is not meaningful. The results of the cloud-to-model assessment using the each of the point clouds as a reference point cloud is shown in Fig.19. The trend that the lower part of the breakwater wall shows significant more and higher difference values is visible in both assessments. This effect is more prominent in the comparison result which uses point cloud 2 as a reference point cloud (bottom). Due to the larger point spacing, the local modelling covers a larger area which leads to larger distance calculations.

This result is also underlined when quantifying the 95% measuring threshold. When the reference point cloud is epoch 1 95% of all measurements are within 0.170m. When the reference point cloud is epoch 2, 95% of all measurements are within 0.297m (Table.6). A difference of over 10cm.

The results when increasing the number of points for the local modelling to 18 is presented in Fig.20. The previously discussed trend of the lower part of the breakwater wall showing significant more and higher difference values is also visible here. When the reference point cloud is epoch 1 then 95% of all measurements are within 0.180m compared to 0.170m when using 6 points for the local modelling. The increased number can be again explained with the larger area used for the local modelling. When the reference point cloud is epoch 2, 95% of all measurements are within 0.307m using 18 points for the local modelling compared to 0.297m when using 6 points for the local modelling. The increase is again around 10cm. All values related to the 95% measurements are summarised in Table.6.

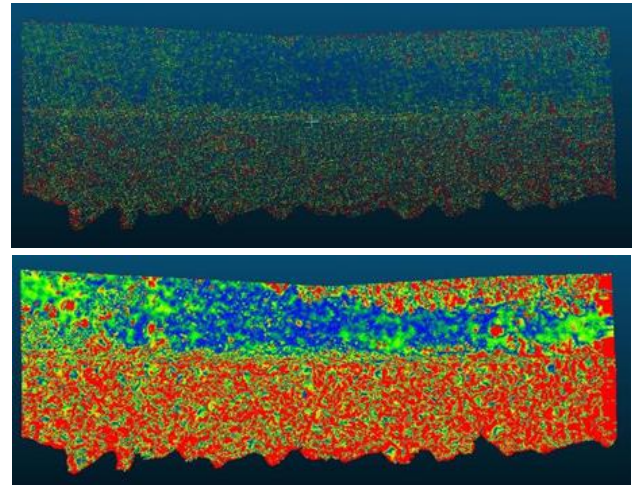


Fig.20. Local Modelling using 12 points. Use of epoch 1 as reference point cloud (top) and use of epoch 2 as reference point cloud (bottom)

Validation as to the cause of the difference is not possible due to different capture, control, and processing methodologies. Variation could be due to physical variation or variation in the data. For this reason, the exercise will be repeated using an identical survey methodology with a new point cloud where precise control point measurements will eliminate data error causing variation.

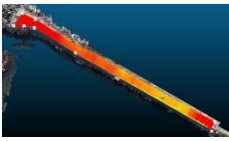
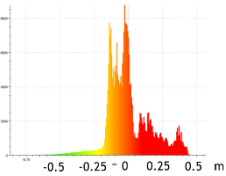
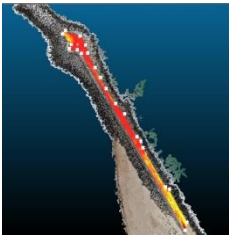
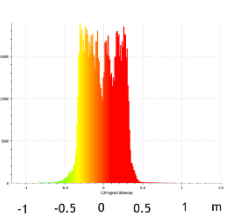
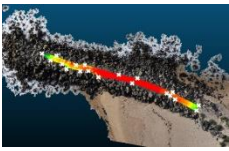
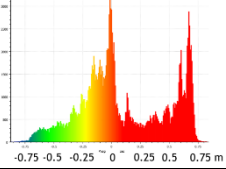
What can be summarised is that the higher density point cloud should be used for the local modelling. Depending on the point spacing and the roughness of the surface the number of points for the local modelling should be chosen carefully as it will impact the results. It will be very likely that armour movement of more than 10cm will be able to be detected which includes armour loss. Loss of armour interlocking can only be detected if there are significant armour rock movements.

Table.6. Summary of all differences within 95% of the observations. All measurements are in [m]

Section of	Reference	Point-to-point	Point-to-Model (k=6)	Point-to-Model (k=18)
Wall 5	Epoch 1	0.111	0.090	0.097
	Epoch 2	0.297	0.103	0.109
Wall 7c	Epoch 1		0.170	0.180
	Epoch 2		0.297	0.307

A more general conclusion is that different water edge lines can introduce false deformation. Different water edge lines can be present if the water level in the port was different during the data capture of the different epochs.

Table.7. Assessment of Breach or loss of crest elevation using a single epoch – Heat Maps and Histograms. The white markers in the Heat Map visualisation are the points used to segment crest points. Colours used in the Heat Map and the histogram indicating the same distances. The y axis of the histogram is the absolute number of points.

	Visualisation (heat map)	Histogram
Inner Harbour Groyne (wall 1)		
Outer Harbour Groyne (wall 7a)		
Outer Harbour Main Breakwater North (wall 7b)		

7. CONCLUSION

This paper presents a proof-of-concept analysis of the assessment of breakwater failure modes using photogrammetry derived point cloud data. The following failure modes which have been investigated are:

- Slope defects
- Breach or loss of crest elevation
- Armour movement or loss/Loss of armour interlocking

The first two failure modes were assessed using the point cloud data from a single epoch only. The main challenge for the slope defect workflow is the manual selection of points along the contours to extract the slope. This is unlikely to be a trivial exercise to be automated. Further investigations are required to assess the use of photogrammetric derived point cloud data for slope changes, so comparison of contours from two different epochs.

The proof-of-concept study showed a high potential for photogrammetry data being able to assess breach or loss of crest elevation. The main challenge faced when modelling the crests was the manual selection of points around the crest's edge. This can be easily overcome by pre-defining a crest polygon, for instance by surveying the crest using GNSS. Further

investigations are required when the aim is not only to quantify relative movements between epochs, but also absolute movements compared to a defined height datum.

Finally, using multiple epoch data, there is a high potential for the use of photogrammetry data for the assessment of armour movement or loss. Further investigations are required for the assessment of loss of armour interlocking. The main challenge when comparing multi-epoch dataset is different point spacing in the epoch data. A cloud-to-model method should be applied. The number of points defined to be used for the local modelling method must be defined based on the armour shapes, sizes and point spacing in the point clouds.

The project could show that timely mapping of breakwater conditions using Unmanned Aerial Vehicles (UAV) and the information derived from the images captured by UAVs is possible for some failure modes. While it is a proof-of-concept study, it is the first step allowing a more automated assessment of breakwater walls.

ACKNOWLEDGMENT

We acknowledge the Southern Ports Authority for their ongoing support of student internship projects and their financial contribution to it. We also want to acknowledge the contributions of J. Paize, G. Pikor and N. Pearson from the Southern Ports Authority in their role as industry advisors as well as Mr Andrew Bell Director of Innovation Central Perth (ICP) for facilitating this project.

REFERENCES

- [1] A. Al-Rawabdeh and A. Habib, "Automated Feature-Based Down-Sampling Approaches for Fine Registration of Irregular Point Clouds", *Remote Sensing*, Vol. 12, No. 7, pp. 1224-1234, 2020.
- [2] P.J. Besl and N.D. McKay, "A Method for Registration of 3-D Shapes", *IEEE Transactions on Pattern Analysis and Machine Intelligence*, Vol. 14, No. 2, pp. 239-256, 1992.
- [3] Cloud Compare Version 2.6.1 User Manual, Available at <http://www.cloudcompare.org/doc/qCC/CloudCompare%20v2.6.1%20-%20User%20manual.pdf>, Accessed at 2022.
- [4] T. Euno and Y. Kobayashi, "Bridge Maintenance, Safety, Management, Life-Cycle Sustainability and Innovations: Breakwater Inspection System using Airbourne LiDAR", Taylor and Francis Group. 2021.
- [5] G. Govare, R. Viquez and H. Alfaro, "Use of Drone Technology and Photogrammetry for Beach Morphodynamics and Breakwater Monitoring", *Coastlab*, Vol. 16, No. 6, pp. 1-8, 2016.
- [6] C. Gomez and H. Purdie, "UAV- Based Photogrammetry and Geocomputing for Hazards and Disaster Risk Monitoring - A Review", *Geoenvironmental Disasters*, Vol. 3, pp. 1-12, 2016.
- [7] D. Gonçalves and U. Andriolo, "On the 3D Reconstruction of Coastal Structures by Unmanned Aerial Systems with Onboard Global Navigation Satellite System and Real-Time Kinematics and Terrestrial Laser Scanning", *Remote Sensing*, Vol. 14, No. 6, pp. 1-15, 2022.

- [8] H. Gonzalez Jorge, B. Conde and P. Arias, "UAV Photogrammetry Application to the Monitoring of Rubble Mound Breakwaters", *American Society of Civil Engineers*, Vol. 30, No. 1, pp. 1-8, 2014.
- [9] E. Grilli and F. Remondino, "A Review of Point Clouds Segmentation and Classification Algorithms", *The International Archives of the Photogrammetry, Remote Sensing and Spatial Information Sciences*, Vol. 2, No. 3, pp. 339-344, 2017.
- [10] P. Helmholz and A. Woods, "The Influence of the Point Cloud Comparison Methods on the Verification of Point Clouds using the Batavia Reconstruction as a Case Study", Archaeopress Publishing Limited, 2020.
- [11] R. Lemos, R. Capitao, C. Fortes and T. Martins, "A Methodology for the Evaluation of Evolution and Risk of Breakwaters", *Journal of Integrated Coastal Zone Management*, Vol. 20, No. 2, pp. 103-119, 2020.
- [12] Bunbury Port Development - Long Term Monitoring and Management Plan, Available at <https://www.southernports.com.au/sites/default/files/2021-09/Bunbury%20Port%20Development%20-%20Long%20Term%20Monitoring%20And%20Management%20Plan%20%28LTMMMP%29.pdf>, Accessed at 2021.
- [13] Open 3D, Available at http://www.open3d.org/docs/release/tutorial/pipelines/icp_registration.html, Accessed at 2023.
- [14] PCL Version 1.11.1, Available at https://pcl.readthedocs.io/projects/tutorials/en/latest/statistical_outlier.html, Accessed at 2023.
- [15] Pix4D, Version 5.0.45, Available at <https://www.pix4d.com/>, Accessed at 2022.
- [16] T. Rabbani and G. Vosselman, "Segmentation of Point Clouds using Smoothness Constraint", *Proceedings of International Symposium on Recent Trends in Computer Science*, pp. 248-252, 2006.
- [17] S. Rusinkiewicz and M. Levoy, "Efficient Variants of the ICP Algorithm", *Proceedings of International Conference on 3-D Digital Imaging and Modeling*, pp. 145-152, 2001.
- [18] R.B. Rusu, "Semantic 3D Object Maps for Everyday Manipulation in Human Living Environments", *KI - Künstliche Intelligenz*, Vol. 24, No. 4, pp. 91-93, 2010.
- [19] Site Scan, "Site Scan for ArcGIS by ESRI", Available at <https://www.esri.com/en-us/arcgis/products/site-scan-for-arcgis/overview>, Accessed at 2022.
- [20] P.J. Sousa and E. Franco, "Structural Monitoring of a Breakwater using UAVs and Photogrammetry", *Procedia Structural Integrity*, Vol. 37, pp. 167-172, 2022.
- [21] A. Tremeau and N. Borel, "A Region Growing and Merging Algorithm to Color Segmentation", *Pattern Recognition*, Vol. 30, No. 7, pp. 1191-1203, 1997.
- [22] United States Army Corps of Engineers, Available at <https://www.publications.usace.army.mil/usace-publications/engineer-manuals/>, Accessed at 2022.
- [23] T. Ueno and Y. Kobayashi, "*Breakwater Inspection System using Airborne LiDAR*", Taylor and Francis Group, 2021.
- [24] H. Woo and K. Lee, "A New Segmentation Method for Point Cloud Data", *International Journal of Machine Tools and Manufacture*, Vol. 42, No. 2, pp. 167-178, 2002.
- [25] Q. Zhan, Y. Liang and Y. Xiao, "Color-Based Segmentation of Point Clouds", *Proceedings of International Workshop on Laser Scanning*, Vol. 38, pp. 1-9, 2009.
- [26] Y. Zhang and S. Chen, "UAV Low Altitude Photogrammetry for Powerline Inspection", *ISPRS International Journal of Geo-Information*, Vol. 6, No. 1, pp. 1-16, 2017.